

## Empirical formulas for calculation of submersion coefficient of vertical pipe in air lift pump

M. Kalenik<sup>1</sup>, P. Wichowski<sup>1</sup>, M. Chalecki<sup>1</sup>, A. Koziol<sup>2</sup>, M. Babych<sup>3</sup>

<sup>1</sup>Department of Civil Engineering; <sup>2</sup>Department of Hydraulic Engineering; <sup>1,2</sup>Warsaw University of Life Sciences WULS-SGGW; Nowoursynowska 159; 02-776 Warsaw;  
e-mail: marek\_kalenik@sggw.pl; piotr\_wichowski@sggw.pl; marek\_chalecki@sggw.pl;  
adam\_koziol@sggw.pl

<sup>3</sup>Department of Energy, Lviv National Agrarian University; e-mail: m.babych@ukr.net

Received September 05.2016; accepted September 14.2016

**Summary.** The paper presents the analysis of results of the investigations concerning a vertical pipe submersion coefficient  $h/L$  with an air-water mixer of the described type. The investigations were performed on an air lift pump testing stand, constructed in a laboratory on a scale of 1:1. At first, the paper presents the possibilities of application of air lift pumps. The investigations to date have been briefly characterized and a research problem formulated. Then the paper describes the construction and working principle of the air lift pump testing stand, constructed in a laboratory. It presents the methodology of derivation of empirical formulas for calculation of vertical pipe submersion coefficients  $h/L$ . The comparative analysis of the values of  $h/L$  determined in the measurements with the values of  $h/L$  calculated using the derived empirical formulas was carried out. The research scope encompassed the derivation of the aforementioned empirical formulas for five fixed values of air lift pump delivery head  $H$ , comparison of the obtained values  $h/L$  determined in the measurements with the values of  $h/L$  calculated using the derived empirical formulas and the improved analytical Stenning-Martin model. To derive the empirical formulas for calculation of the vertical pipe submersion coefficient  $h/L$ , the dimensional analysis and multiple regression was applied. The investigations of the vertical pipe submersion coefficient  $h/L$  were carried out for the vertical pipe internal diameter  $d = 0.04$  m and for the fixed delivery heads  $H$ : 0.45, 0.90, 1.35, 1.80, 2.25 m. The values calculated using the derived empirical formulas (23), (24), (25), (26), (27) coincide with the values of  $h/L$  determined in the measurements for the whole range of the investigated delivery heads  $H$ . On the other hand, the values of  $h/L$  calculated using the improved analytical Stenning-Martin model do not coincide with the values of  $h/L$  determined in the measurements for the delivery heads  $H$  equal 0.45 and 0.90 m, whereas they are comparable for  $H$  equal 1.35, 1.80, 2.25 m. For the tested air lift pump with the air-water mixer of the described type (Fig. 2), the maximum air pressure should not exceed  $p_p = 145$  kPa, because for higher pressures the water flow rate diminishes. In the air lift pump being tested, the water flow rate  $Q_w$  grows along with the rise in the air flow rate and in the vertical pipe submersion coefficient  $h/L$  whereas falls along with the rise in the delivery head  $H$ .

**Key words:** air lift pump, two-phase flow, air-water mixer, vertical pipe submersion coefficient.

### INTRODUCTION

Nowadays in Poland, air lift pumps are used to lift sewage and sewage sediments in small near-home container sewage-treatment plants and big group sewage-treatment plants [1] as well as in high-rate filters with self-regenerating bed [2] or for renovation of bored wells. However, in the world, the air lift pumps have much wider application. They are used to aerate and mix water as well as to remove carbon dioxide from water in industrial fish farmings [3], to mix water in deep lakes and to aerate it by means of transport of water from the lake bed onto its surface [4, 5]. Due to the simple construction and high reliability of the air lift pumps, they are applied in various branches of industry, especially in the petrochemical industry to raise oil from dead wells [6], in the chemical industry to transport corrosive, radioactive, arid or toxic fluids [7, 8] as well as to pump boiling fluids, where the change of liquid phase into gas phase occurs [9]. They are also used to transport suspensions in mining industry and to lift manganese concretions from deep seabed up to ca. 4000-6000 m [10].

A two-phase (liquid-gas) or three-phase (liquid-gas-solid) flow exists in the air lift pumps which – as it arises from the performed investigations – is very difficult for mathematical modeling, for it depends on many factors and variables [10-13]. The hydraulic operating conditions of two- and three-phase flow in the air lift pumps are very poorly identified [8]. There are made some attempts to identify flow structures, occurring in various conditions of liquid-gas flow or liquid-gas-solid flow, and to work out so-called flow structure maps for them and mathematical models for simulation of flows occurring in the air lift pumps [4, 6-8, 14-20].

The tests of air lift pumps built of rectangular [21] and curved [22] pipes were also carried out. The performed investigations of the air lift pumps with the curved pipes behind the air-water mixer show that the pumping efficiency of solid bodies significantly falls in such air lift pumps. However, if only liquid is being pumped then the curvature of the pipe of the air lift pump does not affect its efficiency [23]. The performed

investigations show that the air lift pumps are characterized by small working efficiency compared to conventional pumps [8,10, 12, 24].

There is few information on principles of the dimensioning and construction of air lift pumps in the accessible scientific and technical literature [25, 26]. Especially, there is no information how to design air-water mixers to obtain the best operating parameters of the air lift pump.

From the investigations to date it arises that the type of an air-water mixer and the diameter of a vertical pipe applied in the air lift pump affect its efficiency and hydraulic operating conditions [4, 6, 9, 10, 13]. The number, diameter and distribution of holes in the air-water mixer has very big influence on the types of structure of two-phase flow of air and liquid in the air lift pump.

However, in aim to analyze the obtained measurement results, the improved analytical Stenning-Martin model will be used which is constructed of the following equations [27]:

$$\frac{h}{L} = \frac{Q_w^2}{2gLA^2} \left[ \left( \frac{fL}{d} + 1 \right) + \left( \frac{fL}{d} + 2 \right) \frac{Q_p}{Q_w} \right] + \frac{1}{1 + \frac{Q_w}{sQ_p}} \quad (1)$$

$$s = 1.2 + 0.2 \frac{Q_p}{Q_w} + \frac{0.35A\sqrt{gd}}{Q_w} \quad (2)$$

$$\frac{1}{\sqrt{f}} = -2 \log \left( \frac{\frac{\varepsilon}{d}}{3.7} + \frac{2.51}{Re\sqrt{f}} \right) \quad (3)$$

$$Re = \frac{(Q_p + Q_w)d}{\nu A} \quad (4)$$

The remaining quantities will be calculated from the equations:

$$\varepsilon = \frac{k}{d} \quad (5)$$

$$A = \frac{\pi d^2}{4} \quad (6)$$

where:  $h/L$  – vertical pipe submergence ratio [-],  $Q_w$  – water flow rate [ $m^3 \cdot s^{-1}$ ],  $Q_p$  – air flow rate [ $m^3 \cdot s^{-1}$ ],  $h$  – vertical pipe submergence length [m],  $L$  – vertical pipe length-to-outlet [m],  $g$  – gravitational acceleration [ $m \cdot s^{-2}$ ],  $d$  – vertical pipe diameter [m],  $s$  – slip ratio [-],  $f$  – friction factor [-],  $\varepsilon$  – relative roughness [-],  $k$  – absolute roughness [m],  $A$  – vertical pipe cross-sectional area [ $m^2$ ],

$Re$  – Reynolds number [-],  $\nu$  – liquid kinematic viscosity [ $m^2 \cdot s^{-1}$ ].

#### THE ANALYSIS OF RECENT RESEARCHES AND PUBLICATIONS

Kassab et al. [14] investigated hydraulic operating conditions of an air lift pump built of a transparent vertical pipe with the length of 3.75 m and internal diameter of 25.4 mm as well as an air-water mixer with 56 holes with the diameter of 3 mm. The holes in the mixer were evenly distributed on the circumference of the vertical pipe in seven rows and eight columns. The water-air mixer was installed in the distance of 20 cm from the lower end of the transparent vertical pipe. The Authors performed their investigations for the vertical pipe submergence ratio  $h/L$  from 0.2 till 0.75 with the interval 0.1 and for the fixed air pressures  $p_p$  from the range  $1.0 \cdot 10^4 \div 2.7 \cdot 10^5$  Pa. The tests encompassed three stages. The first one consisted in experimental investigations of two-phase flows occurring in the constructed air lift pump. The Authors investigated there the efficiency  $\eta$  of the air lift pump and how the water flow rate  $Q_w$  of the pump changes in the dependence on changes of the vertical pipe submergence ratio  $h/L$  and the fixed air pressure  $p_p$  as well as what structures of two-phase flows occur there. In the second stage, they modified the Stenning-Martin model and worked out a computer program to simulate the water flow rate  $Q_w$  in the air lift pump being tested. The third stage encompassed simulation tests of the water flow rate  $Q_w$  using the created computer program and the comparison of the results obtained there with those obtained in the experimental tests. The performed tests showed that the created computer program basing on the modified Stenning-Martin model can be successfully applied to forecast the water flow rate  $Q_w$  in the air lift pump with the air-water mixer applied there by the Authors.

Kim et al. [15] investigated hydraulic operating conditions of air lift pumps built of transparent vertical pipes with the internal diameters of 8, 11 and 18 mm and of air-water mixers with one-point introduction of air through the lower ends of the vertical pipes. The range of the investigations were performed for three values of vertical pipe submergence ratio  $h/L$ : 0.8, 0.9, 1.0. They encompassed three stages. In the first one, using the results of investigations of hydraulic operating conditions of air lift pumps obtained by other researchers, the Authors proposed a theoretical model to calculate flow rate of the air lift pumps. In the second stage, they performed experimental tests of the dependence between the water flow rate  $Q_w$  in air lift pumps and the fixed air flow rate  $Q_p$  and they recognized the two-phase flow structures occurring in the vertical pipes as the air flow rates  $Q_p$  were being set. The obtained measurement results of the water flow rate  $Q_w$  were compared by the Authors to the calculations carried out using the constructed theoretical model. For the vertical pipe diameters and submergence ratios being tested, the values of water flow rate  $Q_w$  from the model did not coincide sufficiently the experimental results. The obtained results showed that the water flow rate  $Q_w$  in air lift pumps depends on the vertical pipe diameter. However, the results obtained in the theoretical model showed that the

vertical pipe diameter does not affect the water flow rate  $Q_w$ . Due to this, the model proposed by the Authors to calculate water flow rates  $Q_w$  in air lift pumps should be improved to the form which would take the vertical pipe diameter into consideration. On the other hand, the Authors showed that the vertical pipe diameter and submergence ratio in the air lift pump does not affect the types of the air-water two-phase flow structures occurring there. The types of the two-phase flow structures in the air lift pumps depend mainly on the air flow rate. Along with the rise in the air flow rate, the two-phase flow structures change in the air lift pumps. Other researchers also confirm that such dependences occur in the air lift pumps [6, 12, 13, 15]. As the air flow rate grows in the air lift pumps, there become to occur: bubbly flow, slug flow, churn flow, annular flow [6, 15].

Khalil et al. [9] investigated the influence of air-water mixers on the flow rate in air lift pumps. The tests were carried out for an air lift pump built of a steel vertical pipe with the length of 200 cm and the internal diameter of 25.4 mm, for nine types of air-water mixers having 1, 2, 3, 4, 6, 15, 25, 34 and 48 bored air injection holes as well as for four vertical pipe submergence ratios  $h/L$ : 0.5, 0.6, 0.7, 0.75. The results of the investigations showed that the air-water mixer type and the vertical pipe submergence ratio significantly affect the flow rate and efficiency of air lift pumps. Almost for all vertical pipe submergence ratios, the highest flow rate was reached by the air lift pump with the mixer with three bored air injection holes. Furthermore it was stated that the three-hole mixer provides the highest water flow velocity for all tested vertical pipe submergence ratios.

Tighzert et al. [24] investigated the influence of a vertical pipe submergence ratio on the water flow velocity and working efficiency of an air lift pump built of a transparent vertical pipe with the length of 3.1 m and the internal diameter of 33 mm. The scope of the investigations encompassed ten submergence ratios  $h/L$ : 0.26, 0.40, 0.52, 0.58, 0.65, 0.71, 0.78, 0.84, 0.90, 0.94. The researchers showed that as the vertical pipe submergence ratio increases then the water flow velocity also rises in the tested air lift pump. Simultaneously, the efficiency of the air lift pump rises along with the increase of the vertical pipe submergence ratio only up to the value of  $h/L = 0.75$ , whereas for higher values of  $h/L$  its efficiency significantly falls. On the other hand, the maximum values of the efficiency of the air lift pump do not coincide the maximum water flow velocity. The efficiency of the air lift pump decreases along with the water flow velocity. The Authors determined the optimum range of the vertical pipe submergence ratio for the tested air lift pump – it is equal  $0.40 \div 0.75$ .

Hanafizadeh et al. [6], using visual techniques, investigated two-phase flow structures occurring in an air lift pump built of a vertical transparent pipe with the length of 6 m and the internal diameter of 50 mm. During the tests, air was injected into the vertical pipe by an air-water mixer with 108 holes with the diameter of 0.5 mm. The researchers recognized and described four types of two-phase flows occurring in the tested air lift pump. They proved that the types of two-phase flow in air lift

pumps vary depending on a set air flow rate. The Authors noted that as the air flow rate rises in the vertical pipe, at first a bubbly flow occurs, then a slug flow, after that a churn flow and at the end – annular flow. However, for small values of submergence ratio  $h/L$  the bubbly flow is not able to lift water upwards due to small buoyant force of individual bubbles. Only for high submergence ratios  $h/L$  the bubbly flow lifts water upwards whereas the remaining types of flow structures lift water upwards in the whole range of the tested submergence ratios  $h/L$ . The Authors concluded that for an air lift pump for liquids the slug flow is the most appropriate.

## OBJECTIVE

The aim of the paper is to present the analysis of results of the investigations of vertical pipe submergence ratio  $h/L$  with the air-water mixer of the described type. The scope of the investigations encompassed: the derivation of empirical formulas for calculation of the vertical pipe submergence ratio  $h/L$  for five fixed water delivery heads  $H$ : 0.45, 0.90, 1.35, 1.80, 2.25 m in the air lift pump with the vertical pipe internal diameter  $d = 0.04$  m; and comparison of the values  $h/L$  obtained in the measurements with those calculated using the derived empirical formulas and the improved analytical Stenning-Martin model.

## DESCRIPTION OF THE AIR LIFT PUMP TESTING STAND

Figure 1 shows the construction and operating principle of the stand for investigations of hydraulic operating conditions of air lift pumps (air lift pump testing stand). The pipeline (5) delivered water to the plastic tank (7) with the capacity of 450 liters after opening of the ball valve (6). During the tests the tank (7) was permanently filled with water up to the height of 1.0 m. After opening of the ball valve (12), the excess of the water being delivered to the tank (7) was carried by the overfall (11) to the sewerage through a floor inlet (15). The draining pipeline (13) served to empty the tank (7) from the water after the ball valve (14) opening.

Inside of the tank (7), at the height of 0.20 m upon its bottom, the transparent plastic vertical pipe (9) with the internal diameter of 0.04 m, the height of 4.0 m and absolute roughness coefficient  $k = 0.001$  mm was mounted. At this vertical pipe (9), the scale (24) was placed to measure air lift pump delivery head. To measure air lift pump delivery rate, five measuring pipe tees (3) were mounted in the vertical pipe (9), at the heights of 0.45 m, 0.90 m, 1.35 m, 1.80 m and 2.25 m measured over the water level in the tank (7). The upper section (1) of the vertical pipe (9) was closed with cork. In the vertical pipe (9), at the height of ca. 0.30 m over its lower edge, the air-water mixer (8) was mounted. To measure water temperature in the tank (7), the electronic thermometer (26) was applied.

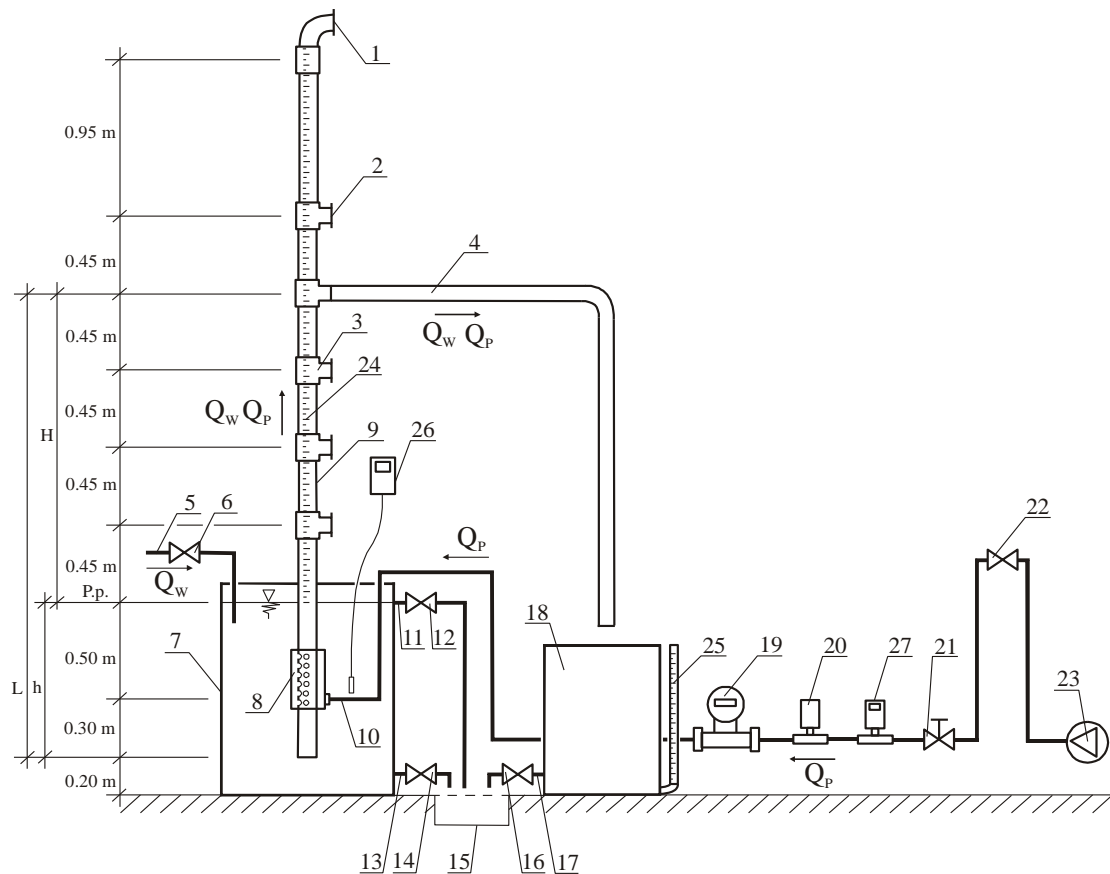


**Fig. 1.** Scheme of the air lift pump testing stand: 1 - delivery pipe, closed with cork, 2 - measuring tee, closed with cork, 3 - measuring tee, 4 - water and air carrying pipe, 5 - water supplying pipe, 6, 12, 14, 16, 22 - ball cut-off valve, 7 - tank, 8 - air-water mixer, 9 - transparent vertical pipe, 10 - air supplying pipe, 11 - overfall, 13, 17 - draining pipe, 15 - floor inlet, 18 - measuring container, 19 - electronic air flow meter, 20 - electronic manometer, 21 - poppet valve, 23 - compressor, 24 - scale, 25 - water-level gauge, 26, 27 - electronic thermometer,  $h$  - vertical pipe submergence length,  $L$  - vertical pipe length-to-outlet,  $H$  - delivery head.

Figure 2 shows a constructive solution of the air-water mixer. The mixer had a form of a mixing chamber (3) with the internal diameter of 0.08 m, tightly fastened on the vertical pipe (1) with the external diameter of 0.05 m. The mixing chamber (3) along with the internal sealing had the external height of 0.30 m and the internal height of 0.25 m. Its width, measured from the external wall of the vertical pipe (1) to the internal wall of the mixing chamber (3), was equal 0.015 m. Inside the mixing chamber (3), in a section of the vertical pipe (1), 75 holes (4) with the diameter of 0.004 m were bored, in five columns and fifteen rows. The holes (4) were placed at the half of circumference of the vertical pipe (1), on the side of the steel end (2) through which the air was pressed into the air lift pump. Such construction caused the pressure stabilization in the mixer chamber in the moment of air delivery to the mixer. It brought on a smooth air delivery through all the holes (4) in one time. The applied steel end (2) through which the air was pressed into the air lift pump had the diameter of 0.015 m. To deliver the air, the elastic pipe (10 at the Fig. 1) was put on the steel end (2).

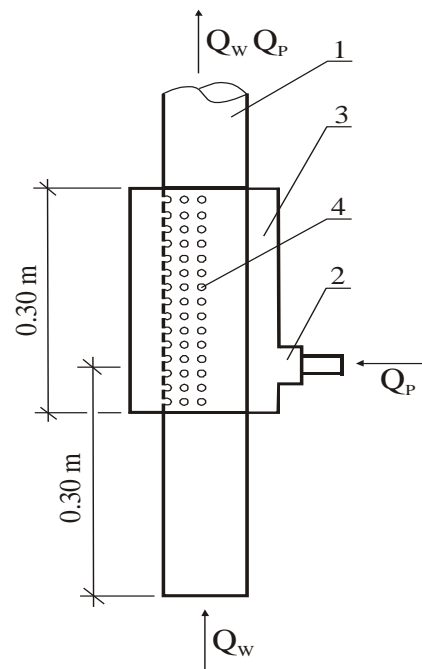


**Fig. 2.** Construction of the air-water mixer: 1 - transparent vertical pipe, 2 - steel end joining the elastic air supplying pipe, 3 - mixing chamber, 4 - holes.

At the pipeline (Fig. 1) with the internal diameter of 0.013 m, delivering the air from the compressor (23) to the air-water mixer (8), the electronic air flow meter (19), electronic manometer (20), poppet valve (21) and ball cut-off valve (22) were mounted.

The investigations were performed with the use of the Endress&Hauser devices. The electronic air flow meter (19) measuring range was 0.0 to 25.0 m<sup>3</sup>·h<sup>-1</sup> and the electronic manometer (20) measuring range – 0.0 to 400 kPa. The measurements concerned water and air temperature, air pressure, barometric pressure, air flow rate and lifted water volume per time unit. The poppet valve (21) was used to regulate the air pressure.

To measure the air lift pump delivery rate, the measuring vessel method was applied, i.e. there was used the plastic measuring tank (18) with the capacity of 80 dm<sup>3</sup> which was scaled at each 0.5 dm<sup>3</sup> to the capacity of 60 dm<sup>3</sup>. The tank capacity scale was put on the transparent water-level gauge (25), mounted at the side of the measuring tank (18). Such solution allowed to read very precisely the volume of the water lifted by the air lift pump per time unit. The lifted water flew down to the measuring tank (18) through the measuring tee (3) and the water carrying pipe (4) with the internal diameter 0.04 m. During the measurements on a given measuring tee (3), the remaining tees were closed with cork (2).

#### METHODOLOGY OF DERIVATION OF THE STRUCTURAL EQUATION

Taking into consideration that the air-water mixture flow structures are very diverse and the work of air lift pumps is very dynamic and various [5, 7, 9, 12-14], it must be stated that it is very hard to work out any classical mathematical model for derivation of a formula for calculation of a vertical pipe submergence ratio  $h/L$  in air lift pumps. Due to this, the dimensional analysis [28-30] was applied to determine the formula. Basing on the performed literature review, on the measurements made on the air lift pump testing stand (Fig. 1) and on the performed analysis of dimensional variables, an assumption was made that the vertical pipe submergence ratio  $h/L$  depends on the following dimensional variables:  $h$  – vertical pipe submergence length [m],  $L$  – vertical pipe length-to-outlet [m],  $Q_p$  – air flow rate [m<sup>3</sup>·s<sup>-1</sup>],  $p_b$  – barometric pressure [kg·m<sup>-1</sup>·s<sup>-2</sup>],  $p_p$  – air pressure [kg·m<sup>-1</sup>·s<sup>-2</sup>],  $d$  – vertical pipe diameter [m],  $Q_w$  – water flow rate [m<sup>3</sup>·s<sup>-1</sup>],  $\rho_w$  – water density [kg·m<sup>-3</sup>],  $\rho_p$  – air density [kg·m<sup>-3</sup>],  $\mu_w$  – water dynamic viscosity [kg·m<sup>-1</sup>·s<sup>-1</sup>],  $\mu_p$  – air dynamic viscosity [kg·m<sup>-1</sup>·s<sup>-1</sup>],  $g$  – gravitational acceleration [m·s<sup>-2</sup>].

In the first approach, the absolute roughness coefficient  $k$  was also taken into consideration. However, the determined dimensionless parameter  $k/d$  is constant and when numerical coefficients to the empirical formulas were being determined using the multiple regression method with application of the STATISTICA package [31], the program rejected the column with the constant value of  $k/d$  because there was no correlation to the remaining dimensionless parameters. Due to this, the absolute roughness coefficient was not taken into considerations in the further calculations. It must be

emphasized that the vertical pipes being applied in air lift pumps are made of PVC or PE where the absolute roughness coefficient is very small (for PVC  $k = 0,02$  mm, for PE  $k = 0,01$  mm). Due to this, the vertical pipe submergence ratio  $h/L$  does not depend on the absolute roughness coefficient  $k$ . Besides, De Cahard and Delhayé also proved in their investigations [7] that the friction coefficient becomes negligible for vertical pipes with the diameter greater than 10 mm.

In technical conditions, the vertical pipes in air lift pumps are applied without thermal insulation, so the temperature of gas (air) and liquid (water) is close to the ambient temperature. Therefore it can be assumed that the gas and liquid temperature is constant along the vertical pipe and the air and liquid flow is isothermal, thus

$$\frac{P}{\rho_p} = const, \quad \frac{P}{\rho_w} = const.$$

Taking the above assumptions into account, the dimensional equation which describes the phenomenon being considered can be written in a form:

$$f\left(\frac{h}{L \cdot Q_p}, p_b, \frac{p_p}{\rho_w}, \frac{p_p}{\rho_p}, \mu_w, \mu_p, d, Q_w, g\right) = 0 \quad (7)$$

There is  $n = 9$  dimensional quantities in this equation and their dimensions contain  $k = 3$  basic units: m, kg, s. According to the Buckingham's  $\Pi$ -theorem, this equation can be transformed to a dependence of  $n - k = 6$  mutually independent dimensionless parameters  $\pi$ . Three quantities were chosen:  $\mu_w, d, Q_w$ , which contain the aforementioned basic units; their dimensional independence was checked below:

$$[kg \cdot m^{-1} \cdot s^{-1}]^{a_1} \cdot [m]^{a_2} \cdot [m^3 \cdot s^{-1}]^{a_3} = b$$

$$kg^{a_1} \cdot m^{-a_1} \cdot s^{-a_1} \cdot m^{a_2} \cdot m^{3a_3} \cdot s^{-a_3} = b$$

$$m^{-a_1+a_2+3a_3} \cdot kg^{a_1} \cdot s^{-a_1-a_3} = [m]^0 \cdot [kg]^0 [s]^0$$

$$-a_1 + a_2 + 3a_3 = 0 \Rightarrow a_2 = 0$$

$$a_1 = 0 \Rightarrow a_1 = 0$$

$$-a_1 - a_3 = 0 \Rightarrow a_3 = 0$$

thus  $a_1 = a_2 = a_3 = 0, \quad b = 1$  (they are dimensionally independent).

The subsequent connection of the remaining five dimensional quantities with the product of the powers of the chosen dimensionally independent quantities allows to determine the dimensionless parameters  $\pi$ :

$$\pi_1 = \frac{h}{L \cdot Q_p} \mu_w^{a_1} d^{a_2} Q_w^{a_3} \quad (8)$$

$$\pi_2 = p_b \mu_w^{b1} d^{b2} Q_w^{b3} \quad (9)$$

$$\pi_3 = \frac{P_p}{\rho_w} \mu_w^{c1} d^{c2} Q_w^{c3} \quad (10)$$

$$\pi_4 = \frac{P_p}{\rho_p} \mu_w^{d1} d^{d2} Q_w^{d3} \quad (11)$$

$$\pi_5 = \mu_p \mu_w^{e1} d^{e2} Q_w^{e3} \quad (12)$$

$$\pi_6 = g \mu_w^{f1} d^{f2} Q_w^{f3} \quad (13)$$

The substitution of these individual quantities and comparison of the power exponents by the basic units of the both sides of the subsequent equations (analogically as during checking of the dimensional independence of the quantities) yields the values of these quantities:

$$\pi_1 = \frac{h Q_w}{L Q_p} \quad (14)$$

$$\pi_2 = \frac{p_b d^3}{\mu_w Q_w} \quad (15)$$

$$\pi_3 = \frac{p_p d^4}{\rho_w Q_w^2} \quad (16)$$

$$\pi_4 = \frac{p_p d^4}{\rho_p Q_w^2} \quad (17)$$

$$\pi_5 = \frac{\mu_p}{\mu_w} \quad (18)$$

$$\pi_6 = \frac{g d^5}{Q_w^2} \quad (19)$$

According to the Buckingham's theorem, the dimensional equation (7) can be written in a form of dimensionless dependence between the parameters  $\pi$ .

$$f(\pi_1, \pi_2, \pi_3, \pi_4, \pi_5, \pi_6) = 0 \quad (20)$$

hence:

$$\pi_1 = f(\pi_2, \pi_3, \pi_4, \pi_5, \pi_6) \quad (21)$$

Substitution of the terms (14)-(19) instead of  $\pi$ , after rearrangement, gives the structural equation:

$$\frac{h}{L} = f\left(\frac{p_b d^3}{\mu_w Q_w}, \frac{p_p d^4}{\rho_w Q_w^2}, \frac{p_p d^4}{\rho_p Q_w^2}, \frac{\mu_p}{\mu_w}, \frac{g d^5}{Q_w^2}\right) \frac{Q_p}{Q_w} \quad (22)$$

As the structural equation (22) had been derived, an experiment was carried out to determine its numerical coefficients.

#### METHODOLOGY OF INVESTIGATIONS OF THE AIR LIFT PUMP

Before each measuring series had begun on the air lift pump testing stand (Fig. 1), an actual barometric pressure  $p_b$  was measured using the electronic manometer (20). Then, on the water-level gauge (25) connected to the measuring container (18), the minimum level of free surface of water in the measuring container (18) was marked by which the stop-watch would be switched on as well as the maximum level of free surface of water by which the stop-watch would be switched off. The level marked on the water-level gauge (25) scale referred to a certain water volume  $V_w$ . The measurement of the air lift pump (Fig. 1) flow rate  $Q_w$  was started from opening of the valves (6, 12), filling the tank (7) with water, turning on the compressor (23) and opening the valve (22) on the pipeline (10) supplying the air-water mixer (8) with air. Then a demanded value of the air pressure  $p_p$  was fixed on the electronic manometer (20) using the poppet valve (20). As the determined air pressure  $p_p$  had been fixed, some quantity of water – depending on the flow rate  $Q_w$  – flew out from the tank (7). To make the measurement reliable, the water level in the tank (7) had to be kept constant. Changes of the submergence of the air-water mixer (8), connected to the water level changes in the tank (7), cause significant changes in the air lift pump flow rate  $Q_w$ . The constant water level in the tank (7) was kept using the valve (6) placed on the pipeline (7) supplying water to the tank (7). Each time the valve (6) was set in the position which balanced the water flux through a determined measuring tee (3). The observations and regulations of the water level in the tank (7) were performed relatively to the level marked with a horizontal line on its internal wall. As these actions were completed and the working conditions of the air lift pump stabilized, the measurement started. At first, for a fixed value of the air pressure  $p_p$ , the air flow rate  $Q_p$  was being read from the electronic air flow meter (19) and the air and water temperature – from the electronic thermometers (26 – water, 27 – air). Then the measuring container (18) was put under the water carrying pipeline (4) which carried the water being lifted which, in turn, was collected in the measuring container (18). When the water-level gauge (25) showed that the free surface of water reached the marked minimum level, the stop-watch was switched on and the measuring container (18) filling time  $t$  was started to be measured – till the moment when the free surface of water reached the marked maximum level and the stop-

watch was switched off. The time  $t$  of filling of the measuring container (18) with the known water volume  $V_w$  was read from the stop-watch. As the time  $t$  had been written out, the measuring container (18) was pulled out from under the water carrying pipeline (4) and emptied by opening the ball cut-off valve (16). Then the ball cut-off valve (16) was closed, a next value of the air pressure  $p_p$  was set on the electronic manometer (20) and a next measurement started. The measurements were carried out for the fixed air pressure  $p_p$  from 110 till 155 kPa with intervals 5 kPa. The water flow rate  $Q_w$  was calculated by dividing the volume  $V_w$  of water being in the measuring container (18) through the filling time  $t$ . During the tests, three measuring series were carried out – for the fixed values of the air pressure  $p_p$  and all five measuring tees (3). The air flow rate  $Q_p$  of the air lift pump was tested for five delivery heads  $H$ : 0.45, 0.90, 1.35, 1.80, 2.25 m, measured relatively to the free surface of water in the tank (7).

### RESULTS OF THE TESTS AND THEIR DISCUSSION

During operation of the air lift pump with the air-water mixer (Fig. 2), the air flow in the transparent vertical pipe was observed in a form of irregular bulbs

which occurred within the whole cross-section of the pipe. The flux of the water being lifted in the air lift pump was almost continuous with hardly visible pulsation. Along with the increase of the air flow rate  $Q_p$ , it could be observed in the transparent vertical pipe that the flux of air bulbs is more and more intensive, the bulbs have more and more irregular shapes and occupy more and more volume in the vertical pipe, creating air-water emulsion.

Fig. 3 presents a distribution of the water flow rate  $Q_w$  in the air lift pump vs. the air flow rate  $Q_p$  and delivery height  $H$ . Analysis of the obtained results allows to state that the water flow rate  $Q_w$  in the air lift pump rises along with the air flow rate  $Q_p$  and it falls along with the increase of the delivery height  $H$ . On the other hand, the measuring points distribute close to each other creating distinct trend lines for individual delivery heights  $H$  and the observed trend (regression) is a quadratic polynomial. The calculated coefficients of determination  $R^2$  from the sample are higher than 0.93 what means that 93% of the value of the water flow rate  $Q_w$  in the air lift pump depends on the air flow rate  $Q_p$  and only 7% of this value depends on other factors, e.g. the water density, air density, gravitational acceleration.

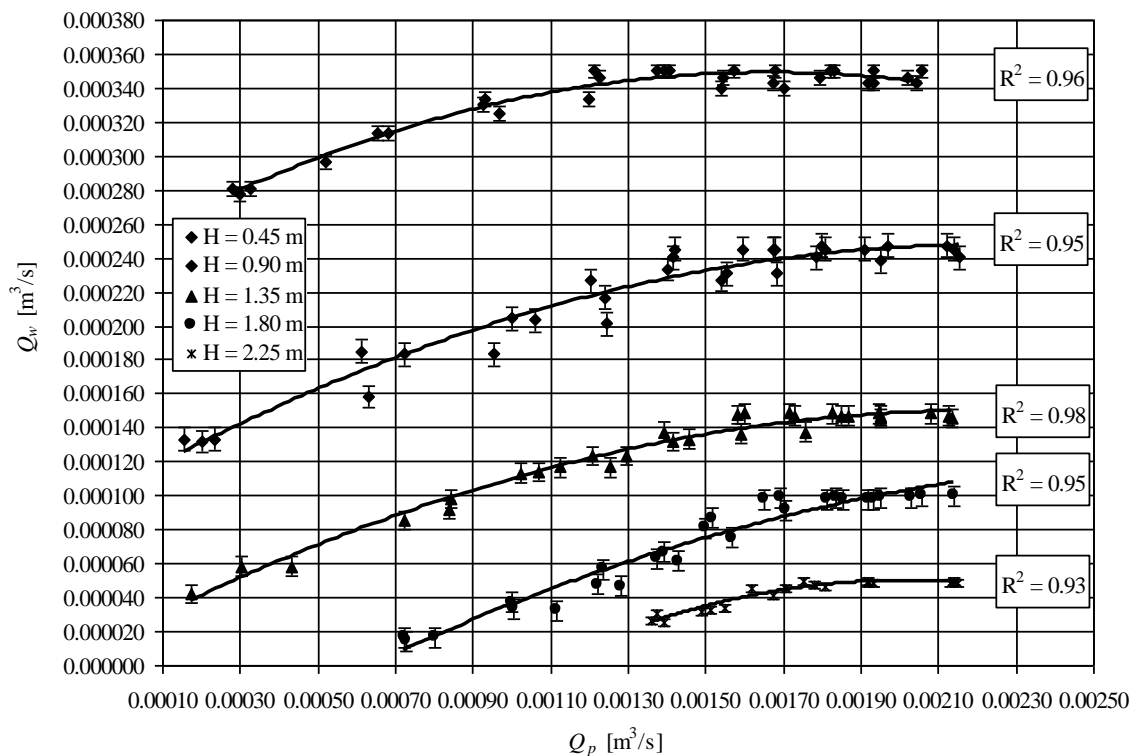


Fig. 3. Water flow rate ( $Q_w$ ) in the air lift pump vs. air flow rate ( $Q_p$ ) and water delivery height ( $H$ ).

To make water flow out from an air lift pump on demanded delivery heights, an appropriate minimum air pressure  $p_{pmin}$  must be guaranteed which is forced by an appropriate air flow rate  $Q_{pmin}$  in a vertical pipe (Fig. 4). As the delivery height  $H$  rises, the demanded minimum air pressure  $p_{pmin}$  rises too and thereby – the air flow rate  $Q_{pmin}$  in the vertical pipe (Fig. 4). In the tested air lift pump (Figs. 1 and 2), for the delivery heights  $H$ : 0.45, 0.90, 1.35 m, the demanded minimum air pressure  $p_{pmin}$  is

equal 110 kPa what is corresponded by the average air flow rate  $Q_{pmin} = 1.25 \text{ m}^3 \cdot \text{h}^{-1}$ ; whereas for the delivery height  $H = 1.80 \text{ m}$   $p_{pmin} = 115 \text{ kPa}$  and  $Q_{pmin} = 2.50 \text{ m}^3 \cdot \text{h}^{-1}$ , for  $H = 2.25 \text{ m}$   $p_{pmin} = 125 \text{ kPa}$  and  $Q_{pmin} = 4.25 \text{ m}^3 \cdot \text{h}^{-1}$ . In the tested air lift pump, as the delivery heights were being still set, when the air pressure  $p_p$  exceeded 145 kPa i.e. the average air flow rate  $Q_{pmin}$  exceeded  $6.50 \text{ m}^3 \cdot \text{h}^{-1}$ , the water flow rate  $Q_w$  of the air lift pump did not rise but started to fall. This

phenomenon is well known and described in the literature [23, 25, 26]. Due to this fact, the maximum demanded air

pressure for the tested air lift pump with the applied (Fig. 2) air-water mixer should not exceed  $p_p = 145$  kPa.

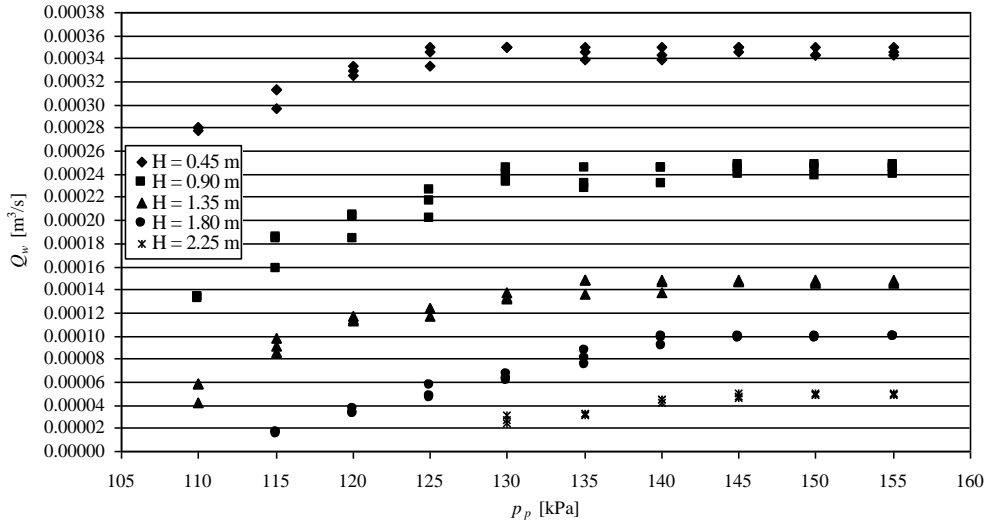


**Fig. 4.** Water flow rate ( $Q_w$ ) in the air lift pump vs. air pressure ( $p_p$ ) and water delivery height ( $H$ )

To determine the vertical pipe submergence ratio  $h/L$ , appropriate empirical formulas were derived. In this aim, using the measurements (Figs. 3 and 4) performed on the air lift pump testing stand (Figs. 1 and 2), the dimensionless parameters  $\pi_1$  (14),  $\pi_2$  (15),  $\pi_3$  (16),  $\pi_4$  (17),  $\pi_5$  (18),  $\pi_6$  (19) were calculated from the derived structural equation (22). Basing on the measured temperatures of water  $T_w$  and air  $T_p$ , the following constants were calculated from the tables [32]: the density of water  $\rho_w$  and air  $\rho_p$ , the dynamic viscosity of water  $\mu_w$  and air  $\mu_p$ . Then appropriate data tables were built and – using the multiple regression method and the computer package STATISTICA [31] – the numerical coefficients to the empirical formulas were determined for the water

delivery heights  $H$ : 0.45, 0.90, 1.35, 1.80, 2.25 m. To determine the coefficients, an additive model of the multiple regression was assumed, because from the performed investigations resulted that the vertical pipe submergence ratio  $h/L$  shows a linear trend. It is the additive model which must be applied when a trend function is linear or transformable to linear. Substitution of the determined numerical coefficients to the structural equation (22) finally yields the following empirical formulas for calculation of the vertical pipe submergence ratio  $h/L$  in air lift pumps (the number of significant digits in the coefficients was reduced for the sake of facilitation in application of these formulas):

- for the water delivery height  $H = 0.45$  m:

$$\frac{h}{L} = \left( -1.25 - 2.46 \cdot 10^{-7} \frac{p_b d^3}{\mu_w Q_w} - 2.26 \cdot 10^{-4} \frac{p_p d^4}{\rho_w Q_w^2} + 1.51 \cdot 10^{-7} \frac{p_p d^4}{\rho_p Q_w^2} + 189.2 \frac{\mu_p}{\mu_w} + 0.318 \frac{g d^5}{Q_w^2} \right) \frac{Q_p}{Q_w} \quad (23)$$

- for the water delivery height  $H = 0.90$  m:

$$\frac{h}{L} = \left( -0.09 - 4.69 \cdot 10^{-8} \frac{p_b d^3}{\mu_w Q_w} - 8.83 \cdot 10^{-4} \frac{p_p d^4}{\rho_w Q_w^2} + 1.045 \cdot 10^{-6} \frac{p_p d^4}{\rho_p Q_w^2} + 51.46 \frac{\mu_p}{\mu_w} + 0.036 \frac{g d^5}{Q_w^2} \right) \frac{Q_p}{Q_w} \quad (24)$$

- for the water delivery height  $H = 1.35$  m:

$$\frac{h}{L} = \left( 0.07 - 1.25 \cdot 10^{-10} \frac{p_b d^3}{\mu_w Q_w} + 1.31 \cdot 10^{-5} \frac{p_p d^4}{\rho_w Q_w^2} - 2.08 \cdot 10^{-8} \frac{p_p d^4}{\rho_p Q_w^2} - 1.66 \frac{\mu_p}{\mu_w} + 1.18 \cdot 10^{-3} \frac{g d^5}{Q_w^2} \right) \frac{Q_p}{Q_w} \quad (25)$$

- for the water delivery height  $H = 1.80$  m:

$$\frac{h}{L} = \left( 0.014 - 3.84 \cdot 10^{-11} \frac{p_b d^3}{\mu_w Q_w} - 1.448 \cdot 10^{-7} \frac{p_p d^4}{\rho_w Q_w^2} - 5.83 \cdot 10^{-10} \frac{p_p d^4}{\rho_p Q_w^2} + 0.6242 \frac{\mu_p}{\mu_w} + 1.807 \cdot 10^{-4} \frac{g d^5}{Q_w^2} \right) \frac{Q_p}{Q_w} \quad (26)$$

- for the water delivery height  $H = 2.25$  m:

$$\frac{h}{L} = \left( 7.9 \cdot 10^{-3} - 3.02 \cdot 10^{-11} \frac{p_b d^3}{\mu_w Q_w} + 6.77 \cdot 10^{-8} \frac{p_p d^4}{\rho_w Q_w^2} - 1.98 \cdot 10^{-10} \frac{p_p d^4}{\rho_p Q_w^2} + 0.28 \frac{\mu_p}{\mu_w} + 3.06 \cdot 10^{-5} \frac{g d^5}{Q_w^2} \right) \frac{Q_p}{Q_w} \quad (27)$$

where:  $h/L$  – vertical pipe submergence ratio [-],  $h$  – vertical pipe submergence length [m],  $L$  – vertical pipe length-to-outlet [m],  $Q_w$  – water flow rate [ $\text{m}^3 \cdot \text{s}^{-1}$ ],  $p_b$  – barometric pressure [ $\text{kg} \cdot \text{m}^{-1} \cdot \text{s}^{-2}$ ],  $p_p$  – air pressure [ $\text{kg} \cdot \text{m}^{-1} \cdot \text{s}^{-2}$ ],  $d$  – vertical pipe diameter [m],  $Q_p$  – air flow rate [ $\text{m}^3 \cdot \text{s}^{-1}$ ],  $\rho_w$  – water density [ $\text{kg} \cdot \text{m}^{-3}$ ],  $\rho_p$  – air density [ $\text{kg} \cdot \text{m}^{-3}$ ],  $\mu_w$  – water dynamic viscosity [ $\text{kg} \cdot \text{m}^{-1} \cdot \text{s}^{-1}$ ],  $\mu_p$  – air dynamic viscosity [ $\text{kg} \cdot \text{m}^{-1} \cdot \text{s}^{-1}$ ],  $g$  – gravitational acceleration [ $\text{m} \cdot \text{s}^{-2}$ ]

Figs. 5, 6, 7, 8, 9 present the results of measurements of the vertical pipe submergence ratio  $h/L$  and its calculations, made using the empirical formulas (23), (24), (25) (26), (27) for the tested delivery heads  $H$ . The analysis of these results allows to state that the water flow rate  $Q_w$  in the air lift pump rises along with the vertical pipe submergence ratio  $h/L$ . The functional dependence between the vertical pipe submergence ratio  $h/L$  and the water flow rate  $Q_w$  is of linear character both for the

values of  $h/L$  obtained from the measurements and from the calculations performed using the empirical formulas (23), (24), (25) (26), (27) as well as the improved analytical Stenning-Martin model formulas. Deviations of the values of  $h/L$  obtained from the calculations with the empirical formulas (23), (24), (25) (26), (27) compared to the values  $h/L$  obtained from the measurements are small for the tested delivery heads  $H$ .

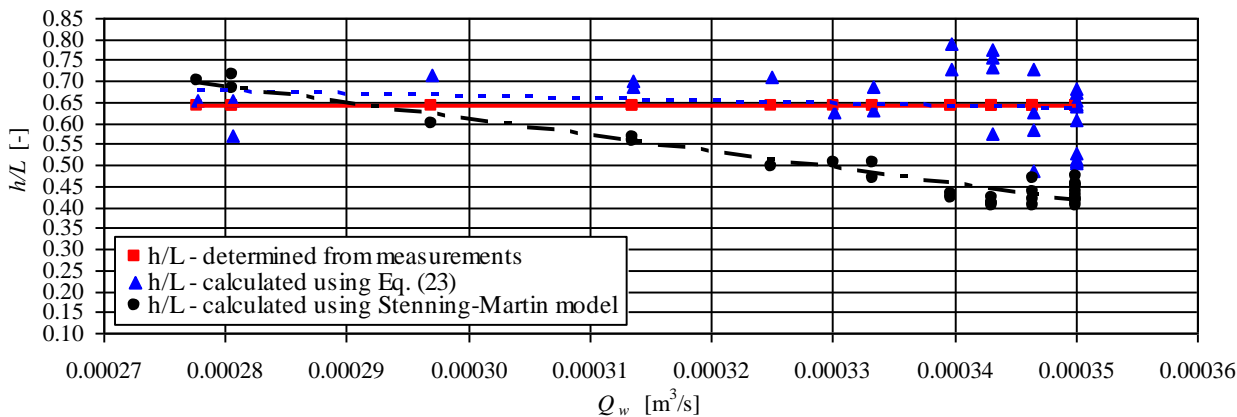


Fig. 5. Vertical pipe submergence ratio ( $h/L$ ) for the delivery head  $H = 0.45$  m

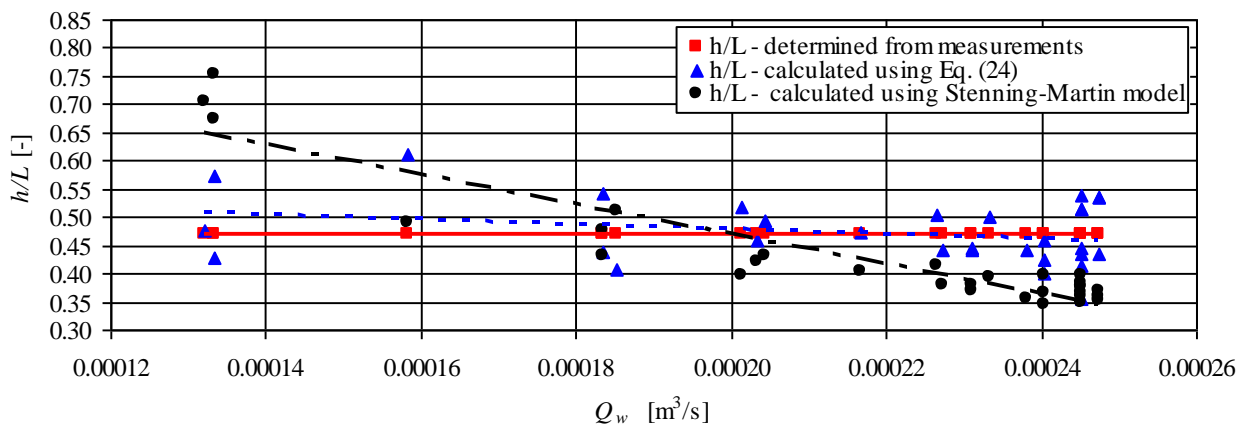


Fig. 6. Vertical pipe submergence ratio ( $h/L$ ) for the delivery head  $H = 0.90$  m

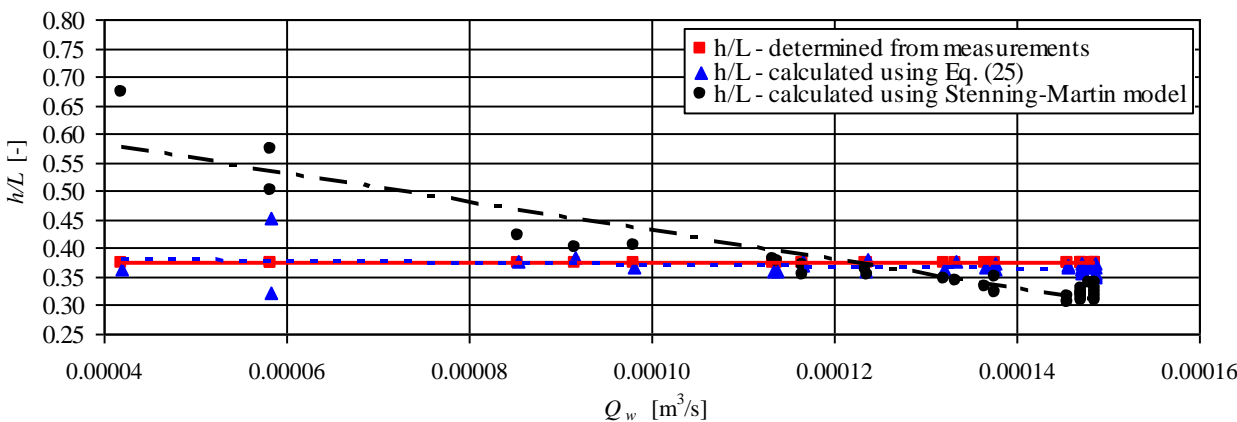


Fig. 7. Vertical pipe submergence ratio ( $h/L$ ) for the delivery head  $H = 1.35$  m

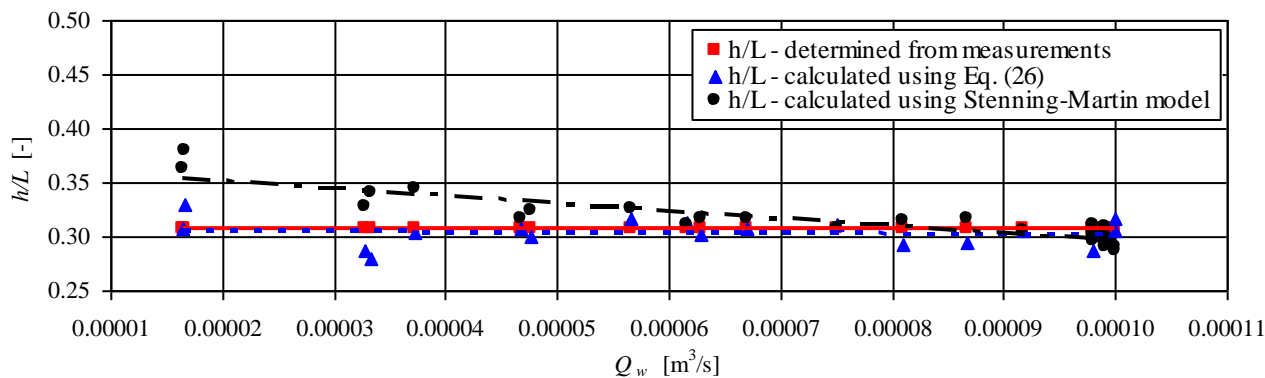


Fig. 8. Vertical pipe submergence ratio ( $h/L$ ) for the delivery head  $H = 1.80$  m

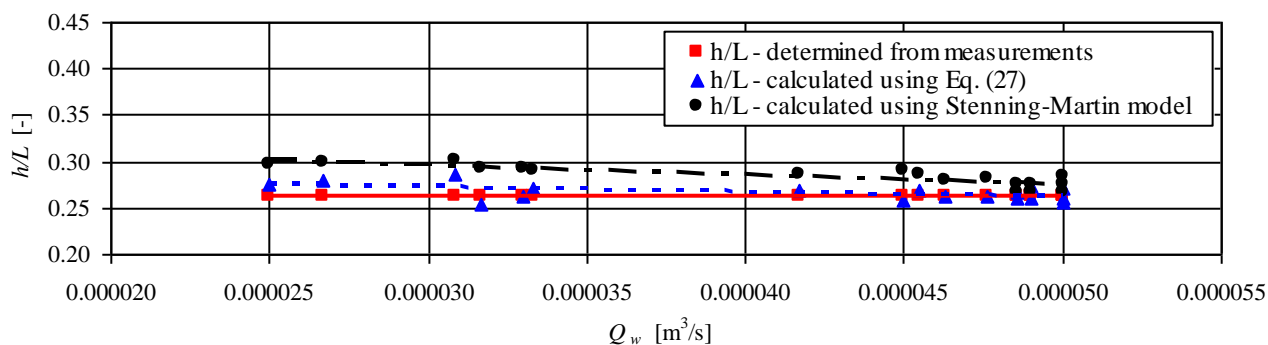


Fig. 9. Vertical pipe submergence ratio ( $h/L$ ) for the delivery head  $H = 2.25$  m

The regression type is linear for the values of the vertical pipe submergence ratio  $h/L$  obtained from the calculations with the empirical formulas (23), (24), (25) (26), (27) and with the improved analytical Stenning-Martin model formulas as well as from those obtained from the measurements. The trend lines for the values of the vertical pipe submergence ratio  $h/L$  obtained from the calculations with the empirical formulas (23), (24), (25) (26), (27) almost coincide with those obtained from the measurements and run almost parallel to each other.

To evaluate the calculation accuracy of the empirical formulas (23), (24), (25) (26), (27), the values  $h/L$  obtained from them and those measured on the air lift pump testing stand were compared. It can be stated that for the parameters:  $d = 0.04$  m,  $110 \text{ kPa} < p_p < 155 \text{ kPa}$ ,  $0.60 \text{ m}^3 \cdot \text{h}^{-1} < Q_w < 21.00 \text{ m}^3 \cdot \text{h}^{-1}$ ,  $1.08 \text{ m}^3 \cdot \text{h}^{-1} < Q_p < 7.76 \text{ m}^3 \cdot \text{h}^{-1}$ ,  $1.2234 \text{ kg} \cdot \text{m}^{-3} < \rho_p < 1.2346 \text{ kg} \cdot \text{m}^{-3}$ ,  $999.0844 \text{ kg} \cdot \text{m}^{-3} < \rho_w < 999.5828 \text{ kg} \cdot \text{m}^{-3}$ ,  $1.1508 \cdot 10^{-3} \text{ kg} \cdot \text{m}^{-1} \cdot \text{s}^{-1} < \mu_w < 1.2048 \cdot 10^{-3} \text{ kg} \cdot \text{m}^{-1} \cdot \text{s}^{-1}$ ,  $1.7730 \cdot 10^{-5} \text{ kg} \cdot \text{m}^{-1} \cdot \text{s}^{-1} < \mu_p < 1.7870 \cdot 10^{-5} \text{ kg} \cdot \text{m}^{-1} \cdot \text{s}^{-1}$ , an average deviation of the value of  $h/L$  does not exceed for the given empirical formula: (23) – 11%, (24) – 10%, (25) – 3%, (26) – 3%, (27) – 2%. The dimensional analysis of the left and right side of these empirical equations was also performed and it showed that the dimensions of both sides of each formula are consistent.

On the other hand, the trend lines for the vertical pipe submergence ratio  $h/L$  calculated according the improved analytical Stenning-Martin model do not coincide with the values of  $h/L$  obtained from the measurements and from the calculations using the empirical formulas (23), (24), (25) (26), (27) – they are strongly sloped towards the

increasing water flow ratio  $Q_w$ . In average, the difference between the values of the vertical pipe submergence ratio  $h/L$  obtained from the measurements and those calculated according the improved analytical Stenning-Martin model does not exceed for the given delivery head:  $H = 0.45$  m – 39%,  $H = 0.90$  m – 23%,  $H = 1.35$  m – 14%,  $H = 1.80$  m – 5%,  $H = 2.25$  m – 7%.

The comparison of the average values of the vertical pipe submergence ratio  $h/L$  obtained from the measurements, those calculated using the empirical formulas (23), (24), (25) (26), (27) as well as calculated using the improved analytical Stenning-Martin model are presented in Table 1.

Table 1. Average values of the vertical pipe submergence ratio.

$H$ [m]	$h/L$ [-]		
	Determined from measurements	Calculated using Eqs. (23), (24), (25), (26), (27)	Calculated with Stenning-Martin model
0.45	0.64	0.65	0.48
0.90	0.47	0.47	0.43
1.35	0.37	0.37	0.37
1.80	0.31	0.30	0.31
2.25	0.26	0.27	0.28

The analysis of Table 1 allows to state that the average values of the vertical pipe submergence ratio  $h/L$  calculated using the empirical formulas (23), (24), (25) (26), (27) coincide with those obtained from the measurements. However, the average values of  $h/L$  obtained from the improved analytical Stenning-Martin model significantly differ from those determined from the measurements for the delivery heads  $H = 0.45$  m and  $H = 0.90$  m, but they are comparable for the delivery heads  $H$ : 1.35, 1.80, 2.25 m.

## CONCLUSIONS

Taking into account that the operating conditions of the tested air lift pump with the air-water mixer presented on Fig. 2 are so very dynamic and changeable, it can be stated that the differences between the values of the vertical pipe submergence ratio  $h/L$  determined from measurements and the values calculated from the empirical formulas (23), (24), (25), (26), (27), are small. The calculated values of  $h/L$  coincide with those determined from the measurements in the whole range of the assumed water delivery heads  $H$ . However, the values of  $h/L$  calculated from the improved analytical Stenning-Martin model for the delivery heads  $H$ : 0.45 and 0.90 m do not coincide with those determined from measurements whereas they are comparable for  $H$ : 1.35, 1.80 i 2.25 m.

For the tested air lift pump with the vertical pipe diameter equal 0.04 m and with the applied mixer (Fig. 2), the water flow rate increases along with the increase of the air pressure from  $p_p = 110$  kPa till  $p_p = 145$  kPa, whereas it starts to fall for higher air pressures. Due to this, the maximum air pressure for the tested air lift pump with the applied mixer (Fig. 2) should not exceed  $p_p = 145$  kPa. The water flow rate in the tested air lift pump increases along with the increase of the air flow rate and vertical pipe submergence ratio  $h/L$  and falls along with the increase of the water delivery head.

## REFERENCES

1. **Tucki K., Sikora M. 2016.** Technical and Logistics Analysis of the Extension of the Energy Supply System with the Cogeneration Unit Supplied with Biogas from the Water Treatment Plant. TEKA. Commission of Motorization and Energetics in Agriculture. Vol. 16, No. 1, 71–76. (In Polish).
2. **Tucki K. 2016.** Use of Solar Collectors on the Example of a Water-Park Part 1: Technical Analysis. TEKA. Commission of Motorization and Energetics in Agriculture. Vol. 16, No. 1, 47–52. (In Polish).
3. **Barrut B., Blancheton J-P., Champagne J-Y., Grasmick A. 2012.** Mass transfer efficiency of a vacuum air lift - application to water recycling in aquaculture systems. Aqua. Eng., 46, 18-26.
4. **Fan W., Chen J., Pan Y., Huang H., Chen C-T. A., Chen Y. 2013.** Experimental study on the performance of air-lift pump for artificial upwelling. Ocean Eng., 59, 47-57.
5. **Parker N.C. 1983.** Airlift pumps and other aeration techniques. In: Water quality in channel catfish ponds, ed. C. S. Tucker, Southern Cooperative Series Bulletin 290. Mississippi Agriculture and Forestry Experiment Station, Mississippi State University, Mississippi, 24-27.
6. **Hanafizadeh P., Ghanbarzadeh, S., Saidi M. H. 2011.** Visual technique for detection of gas-liquid two-phase flow regime in the air lift pump. J. Pet. Sci. Eng., 75, 327-335.
7. **De Cachard F., Delhaye J. M. 1996.** A slug-churn flow model for small-diameter airlift pumps. Int. J. Multiph. Flow, 22, 627-649.
8. **Kassab S. Z., Kandil H. A., Warda, H. A., Ahmedb W. H. 2007.** Experimental and analytical investigations of airlift pumps operating in three-phase flow. Chem. Eng. J., 131, 273-281.
9. **Khalil M. F., Elshorbagy K. A., Kassab S. Z., Fahmy R. I. 1999.** Effect of air injection method on the performance of an air lift pump. Int. J. Heat Fluid Flow, 20, 598-604.
10. **Kalenik M. 2015.** Investigations of hydraulic operating conditions of air lift pump with three types of air-water mixers. Ann. Warsaw Univ. Life Sci. – SGGW, Land Reclam., 47, 1, 69-85.
11. **Kalenik M. 2015.** Empirical formulas for calculation of negative pressure difference in vacuum pipelines. Water, 7, 10, 5284-5304.
12. **Kalenik M. 2015.** Model o fair-lift pump efficiency. Ochr. Sr., 37, 4, 39-46. (In Polish).
13. **Kalenik M., Przybylski P. 2011.** Experimental investigations of hydraulic working conditions of air lift pump. Gaz Woda i Tech. Sanit., 6, 219-223. (In Polish).
14. **Kassab S. Z., Kandil H. A., Warda, H. A., Ahmed, W. H. 2009.** Air-lift pumps characteristics under two-phase flow conditions. Int. J. Heat Fluid Flow, 30, 88-98.
15. **Kim, S. H., Sohn, C. H., Hwang J. Y. 2014.** Effects of tube diameter and submergence ratio on bubble pattern and performance of air-lift pump. Int. J. Multiph. Flow, 58, 195-204.
16. **Mahrous, A-F. 2014.** Performance of airlift pumps: single-stage vs. multistage air injection. Am. J. Mech. Eng., 2, 1, 28-33.
17. **Mahrous A.-F. 2013.** Performance study of an air-lift pump with bent riser tube. Wseas Trans. Appl. Theor. Mech. 8, 2, 136-145.
18. **Mahrous A-F. 2012.** Numerical Study of Solid Particles-Based Airlift Pump Performance. Wseas Trans. Appl. Theor. Mech., 7, 3, 221-230.
19. **Meng, Q., Wang, C., Chen, Y., Chen, J. 2013.** A simplified CFD model for air-lift artificial upwelling. Ocean Eng., 72, 267–276.
20. **Yoshinaga T., Sato Y. 1996.** Performance of an air-lift pump for conveying coarse particles. Int. J. Multiph. Flow, 22, 2, 223-238.
21. **Esen I. I. 2010.** Experimental investigation of a rectangular air lift pump. Adv. Civil Eng., Artical ID 789547.
22. **Fujimoto H., Murakami S., Amura A., Takuda H. 2004.** Effect of local pipe bends on pump performance of a small air-lift system in transporting solid particles. Int. J. of Heat Fluid Flow, 25, 996-1005.

23. **Mahrous A-F. 2013.** Experimental study of airlift pump performance with s-shaped riser tube bend. I.J. Eng. Manu. 1, 1-12.
24. **Tighzert H., Brahimi M., Kechroud N., Benabbas F. 2013.** Effect of submergence ratio on the liquid phase velocity, efficiency and void fraction in an air-lift pump. J. Pet. Sci. Eng., 110, 155-161.
25. **Jankowski F. 1975.** Pumps and Ventilators in Sanitary Engineering. Warsaw, ARKADY. (In Polish).
26. **Wurts W. A., McNeill S. G., Overhults D. G. 1994.** Performance and design characteristics of air lift pumps for field applications. World Aqua., 25, 4, 51-55.
27. **Wahba E.M., Gadalla M.A., Abueidda D., Dalaq A., Hafiz H., Elawadi K., Issa R. 2014.** On the performance of air-lift pumps: from analytical models to large eddy simulation. J. Fluids Eng., 136, 11, 111301: 1-111301:7.
28. **Kasprzak W., Lysik B. 1988.** Dimensional Analysis. Algorithmic Procedures of Experiment Service. WNT. Warsaw 244 p. (In Polish).
29. **Kokar M. 1979.** Determination of mathematical model form with use of dimensional analysis. Inz. Chem., 9, 2, 361-369. (In Polish).
30. **Muller L. 1983.** Application of Dimensional Analysis in Investigations of Models. PWN, Warsaw 245 p. (In Polish).
31. **Statistica 6, 2006.** Computer Program. StatSoft Polska Sp. z o. o., Poland, Cracow.
32. **Orzechowski Z., Prywer J., Zarzycki R. 2001.** Problem Book of Fluid Mechanics in Environmental Engineering. WNT, Warsaw 379 p. (In Polish).

EMPIRYCZNE WZORY DO OBLICZANIA  
WSPÓŁCZYNNIKA ZANURZENIA PIONOWEJ  
RURY W POWIETRZNYM PODNOŚNIKU

M. Kalenik, P. Wichowski, M. Chalecki,  
A. Kozioł, M. Babych

**Streszczenie.** W artykule przedstawiono analizę wyników badań współczynnika zanurzenia pionowej rury  $h/L$  z zastosowanym mieszaczem powietrzno-wodnym. Badania wykonano na stanowisku pomiarowym do badania powietrznych podnośników, wybudowanym w laboratorium w skali 1:1. W artykule przedstawiono zastosowania powietrznych podnośników.

Scharakteryzowano przegląd dotychczasowych badań i sformułowano problem badawczy. W pracy podano budowę i zasadę działania, wybudowanego w laboratorium stanowiska pomiarowego do badania powietrznego podnośnika. Przedstawiono metodykę wyznaczenia empirycznych wzorów do obliczania współczynnika zanurzenia pionowej rury  $h/L$ . Przeprowadzono analizę porównawczą wartości  $h/L$  wyznaczonych z pomiarów, z wartościami  $h/L$  obliczonymi za pomocą wyznaczonych empirycznych wzorów. Zakres badań obejmował wyprowadzenie empirycznych wzorów do obliczania współczynnika zanurzenia pionowej rury  $h/L$  dla pięciu zadanych wysokości podnoszenia wody  $H$  w powietrznym podnośniku, porównanie otrzymanych wartości  $h/L$  wyznaczonych z pomiarów, z wartościami  $h/L$  obliczonymi za pomocą wyprowadzonych empirycznych wzorów i udoskonalonego analitycznego modelu Stenninga i Martina. Do wyznaczenia empirycznych wzorów do obliczania współczynnika zanurzenia pionowej rury  $h/L$  zastosowano analizę wymiarową i metodę regresji wielokrotnej. Badania współczynnika zanurzenia pionowej rury  $h/L$  powietrznego podnośnika wykonano dla średnicy wewnętrznej pionowej rury  $d = 0.04$  m i dla zadanych wysokości podnoszenia wody  $H$ : 0.45, 0.90, 1.35, 1.80, 2.25 m. Obliczone wartości  $h/L$  za pomocą wyznaczonych empirycznych wzorów (23), (24), (25), (26), (27), pokrywają się z wartościami  $h/L$  wyznaczonymi z pomiarów w całym zakresie dla badanych wysokości podnoszenia wody  $H$ . Natomiast wartości  $h/L$  obliczone za pomocą udoskonalonego analitycznego modelu Stenninga i Martina dla wysokości podnoszenia wody  $H$ : 0.45 i 0.90 m nie pokrywają się z wartościami  $h/L$  wyznaczonymi z pomiarów, a dla  $H$ : 1.35, 1.80 i 2.25 m są zbliżone. Dla badanego powietrznego podnośnika z zastosowanym mieszaczem powietrzno-wodnym (rys. 2), maksymalne wymagane ciśnienie powietrza nie powinno przekraczać  $p_p = 145$  kPa, ponieważ dla wyższych ciśnień powietrza natężenie przepływu wody zaczyna spadać. W badanym powietrznym podnośniku natężenie przepływu wody  $Q_w$  rośnie wraz ze wzrostem natężenia przepływu powietrza i wzrostem współczynnika zanurzenia pionowej rury  $h/L$ , a maleje wraz ze wzrostem podnoszenia wody  $H$ .

**Słowa kluczowe:** powietrzny podnośnik, przepływ dwufazowy, mieszacz powietrzno-wodny, współczynnik zanurzenia pionowej rury.